2019 International Conference on Robotics and Automation (ICRA)
Palais des congres de Montreal, Montreal, Canada, May 20-24, 2019

Consolidated control framework to control a powered transfemoral prosthesis over inclined terrain conditions

Woolim Hong[1], Victor Paredes[2], Kenneth Chao[1], Shawanee Patrick[1] and Pilwon Hur[1,*]

Abstract— **For amputees, walking on sloped surfaces is one of the most challenging tasks in their daily lives. Unfortunately, designing a prosthesis that can effectively adapt to varying terrain is an ongoing problem. In this paper, we propose a unified control scheme that enables a powered transfemoral prosthesis to perform human-like walking on sloped terrains regardless of the slope and without any knowledge of the upcoming slope. The control scheme implements impedance control and trajectory tracking during the stance and swing phase, respectively. In the impedance control scheme, properly tuned impedance parameters are used to provide a stable and compliant stance phase that adapts to the slope of the ground. During the swing phase, the system is controlled by a Proportional-Derivative (PD) controller to track the desired trajectories based on cubic Bezier polynomials. These trajectories were obtained by solving an offline optimization problem compared to human slope walking data. Any slope walking trajectories can be generated online by using the optimized Bezier coefficients. At the terminal swing phase, a low gain PD controller is utilized to adapt to the unexpected terrains and smoothly track the generated trajectories. The proposed control framework is implemented on a powered transfemoral prosthesis, *AMPRO II*, on various slopes. The results validate the controller's ability to adapt to terrain inclinations within the range of $\pm 10^{\circ}$.**

I. INTRODUCTION

Amputation can have a negative impact on patients, psychologically and physically. In particular, lower limb amputation results in the reduction of amputees' mobility and dexterity in their daily living – making patients vulnerable to fall and injury [19]. According to the National Center for Health Statistics, transfemoral amputees account for 18.5% of more than 1.2 million amputees in the United States [21]. This makes transfemoral amputees the second largest group among the lower limb amputations [3], [4]. Transfemoral amputees have increased difficulties compared to able-bodied individuals and transtibial amputees due to missing two major joints of articulation. Particularly, slopes can cause problems with gait and balance for transfemoral amputees [9]. In order for amputees to walk successfully on slopes they must make energy compensations to their gait [6], [13], [29] – a mighty task for transfemoral amputees who are missing vital muscles, have limited range of motion, and likely have limited push off from their prosthesis [12], [13], [15], [16], [29].

[1]J. Mike Walker '66 Department of Mechanical Engineering, Texas A&M University, College Station, TX 77843, USA. ulim8819@tamu.edu, kchao@tamu.edu, spatrick2012@gmail.com, pilwonhur@tamu.edu

[2]LimaBionics, Jr. Daniel Carrion 265, Lima 17, Lima, Peru. pvictorm6@gmail.com

[*]Corresponding author

Thus, transfemoral prostheses need to perform stable human-like locomotion under circumstances such as flat-ground and sloped terrains. However, existing passive and micro-processor prostheses have fallen short in achieving this goal. Therefore, there have been several studies on powered transfemoral prostheses, specifically in designing controllers that can emulate human-like gait. A powered transfemoral prosthesis developed by Vanderbilt University, based on impedance control, uses a set of impedance parameters derived from the user's walking gait [22]. Although the device performs well under diverse walking conditions, it mandates a rigorous tuning process by incorporating user-feedback and joint sensors during walking trials [10], [23]. Zhao *et al.,* proposed Human-Inspired Control to avoid the tuning process by using mathematically optimized human-like walking functions [32]. This control scheme also has the advantage of being mathematically stable due to Partial Hybrid Zero Dynamics (PHZD) [1], [32]. However, to generate the trajectories for different walking scenarios while satisfying PHZD conditions, the optimization problem becomes difficult to solve in real-time because of the optimization complexity. To overcome this difficulty, a previous study using convex optimization based spline generation was proposed to generate upslope and flat-ground walking trajectories in real-time [14]. The advantage of this method is the ability to perform flat-ground and upslope walking without any slope information. This is done by adapting to the slope with low gain PD control and blending into the flat-ground walking trajectory with spline generation. However, this method is not applicable to downslopes since the associated walking trajectories vary greatly from those of upslope walking. Specifically, downslope walking demands more knee flexion to avoid foot strikes [12]. In an attempt to enable both upslope and downslope walking, a study using Principal Component Analysis (PCA) was conducted to generate walking trajectories [7]. The results provide a basis for performing real-time slope walking using a lower-dimensional information set. However, this solution requires the detection of slope angle beforehand. Another attempt to overcome the difficulty of sloped walking was conducted using a human-inspired phase variable [17]. This method avoids switching the controller depending on the walking conditions and allows the prosthesis to continuously synchronize with the user's gait. This approach provides a control framework without any additional tuning process according to the walking conditions, such as different gait speeds or upslopes and downslopes. However, for the downslope walking, the prosthetic walking results are provided only

on the small gradients. Hence, in our work, we propose a new approach that would have to cover all slope conditions while minimizing the number of required sensors and heavy optimization in real-time. This is achieved using a single set of impedance and control gain parameters as well as Bezier polynomials to provide proper walking trajectories for all slopes. In addition, by solving an offline optimization problem without having knowledge of slope, we can propose a unified control scheme regardless of the slope. Details are presented as follows; in Section II, the underlying background knowledge is described such as human walking phase and joint kinematic observations on the slopes. Based on the findings from human walking, the proposed method is presented in Section III. The customized powered transfemoral prosthetic system is explained to validate the proposed idea, and the experimental results are shown and discussed in Section IV and V, respectively.

II. PROSTHESIS CONTROL STRATEGIES BASED ON HUMAN WALKING OBSERVATION

Though individuals have different heights and limb lengths, they all share a definite pattern [12] due to the kinematic traits of human walking. In this section, the underlying knowledge of this shared human locomotion such as the human walking phases and the joint kinematic observation is presented. In addition, the proper control strategies and the walking phase detection are discussed for making the prosthetic system mimic human walking.

A. Human walking phases

In order to study the aforementioned human walking pattern, it is necessary to detect the walking phase. Human locomotion is a complex behavior consisting of several events, such as heel-strike (HS), flat-foot (FF), push-off (PO), and toe-off (TO) [25]. Considering these events, human gait can be discretized into finite phases. In this study, human gait was considered to consist of two walking phases: i) stance phase lasting from HS to PO and ii) swing phase lasting from PO to another HS (Fig. 1). The stance phase is commonly specified from 0% to 60% of a gait cycle, and the swing phase is specified from 60% to 100% of the cycle [25].

B. Human locomotion observation on the sloped surfaces

To observe the joint kinematic traits for human locomotion on sloped surfaces, we collected human walking data with a motion capture system (9 Oqus 210c cameras, Qualisys North America, Inc.). A subject (able-bodied male, 28 years, 5'7" height, 150lb weight) walked on a treadmill while the joint kinematics were captured by 14 reflective markers placed on the subject's body as illustrated in Fig. 2 [24]. During the test, the inclination of the treadmill was varied among seven different angles, from -15° to 15° in increments of 5°. We set the limit of the slope angle at ±15° since the angles exceeding ±15° are rarely encountered in daily living.

According to the motion capture results, illustrated in Fig. 1, the patterns of human slope locomotion can be described for different terrain conditions as follows. The following

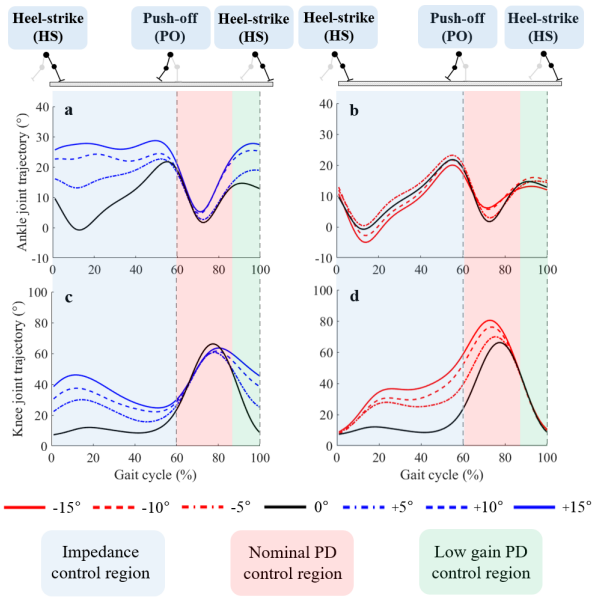

Fig. 1: The ankle (a,b) and knee (c,d) slope walking trajectories for seven different slopes. Black lines indicate flat-ground walking trajectories while blue and red lines indicate upslope and downslope walking trajectories, respectively. The shaded regions describe the different control algorithms according to the different walking phases. A single gait cycle is defined from HS to another HS in percentage terms.

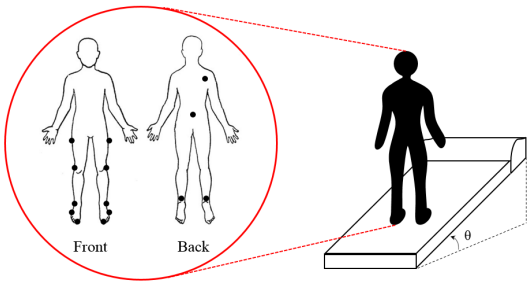

Fig. 2: During the data collection using a motion capture system, 14 reflective markers were put on the subject's body: right and left shoulder, hip, knee, ankle, heel, toe, toe bone, and the left side of the back.

walking trends are also validated by different studies [12], [14], [17].

- **Flat-ground:** The ankle dorsiflexion occurs before HS and plantar-flexion occurs during PO (Fig. 1a,b black-lines). Likewise, the knee joint also undergoes angular deflections: slight flexion and extension after HS, and extensive flexion and extension during the swing phase (Fig. 1c,d black-lines).
- **Upslope:** The ankle joint angle increases with respect to the slope increment in the range of 0% - 60% and 80% - 100% of the gait cycle. On the other hand, in the mid-range of the gait cycle, all ankle deflections tend to converge to the flat-ground trajectory regardless of the

surface's inclination (Fig. 1a blue-lines). An identical trend was observed in the knee deflections (Fig. 1c blue-lines).

- **Downslope:** The ankle joint angles remain the same as those of flat-ground walking regardless of the inclination angles (Fig. 1b red-lines). On the other hand, the knee joint angles deviate from the flat-ground trajectory as the downslope angle grows steeper (Fig. 1d red-lines).

C. Robotic strategy over sloped surfaces

In order to mimic the natural gait of humans on the sloped surfaces above, it is important to decide on a proper control framework for the prosthetic system. In this study, two primary methods are applied to the prosthetic system: i) during the stance phase, the prosthesis is controlled using impedance control that uses parameters derived from the human gait cycle (Fig. 1 blue-shade), while ii) PD control is implemented during the swing phase to track the desired trajectories (Fig. 1 red-shade). At the terminal swing phase, low PD gain parameters are used to make the prosthesis adapt to different terrains without any conflicts (Fig. 1 green-shade). As it is shown in the figure, during the early to mid-swing phase (60% - 85%) of the downslope walking cycle, the knee joint angle trajectories vary considerably with the inclination angle. Note that if the knee flexion of the prosthesis is not large enough while walking downslope, the user may stumble. On the contrary, upslope walking trajectories for the same section of the gait cycle show that the ankle and knee joint angle trajectories conform to the flat-ground walking trajectory (Fig. 1). To generate the proper trajectories with respect to any inclination, Bezier curves were utilized during the early-mid-swing phase; this is discussed in Section III.

D. Human gait synchronization

To achieve stable walking while using the prosthesis, it is crucial to make the prosthetic system synchronize with the user's kinematics during the locomotion. Such synchronization would enable the detection of the user's walking progression and provide the appropriate control signal to follow the proper trajectory. In order to achieve this goal, we are using a phase variable which is widely utilized in the field of robotics [14], [17], [32]. Using the phase variable enables accurate detection of the stage of the gait cycle without having to consider the time that has elapsed.

The phase variable candidates are known to be monotonic; i.e., they are mapped into the gait cycle in a one-to-one manner [26]–[28]. According to the previous research [26], [27], the thigh angle in a global coordinate frame is stated as a good candidate for a phase variable. The change of the global thigh angle can be assumed to be a cosine-like function that has the same periodicity as the human walking gait cycle (i.e., $\theta_{th} \approx Acos(\omega t)$, where ω is referring to walking speed). To satisfy the condition for its monotonic trend, the thigh angle and its integral ($\int \theta_{th}(\tau)d\tau \approx Bsin(\omega t)$) together are used to create the phase variable ($\Phi := arctan(\frac{\int \theta_{th}(\tau)d\tau}{\theta_{th}})$). Before using the thigh angle to compute the phase variable, a normalization process is needed because the variation of thigh angle is different for each step. Therefore, to make the phase variable vary within the bounded range, we propose to normalize the thigh angle using the updated range from the most recent gait.

However, this phase variable still has a limitation since the thigh angle profile is not an ideal cosine function and the normalization process uses the previous step information. To make the walking phase detection more improved, five force sensors (toe: 2, mid-foot: 2, heel: 1) at the bottom of the prosthetic foot are utilized along with the phase variable; the foot-rolling motion can also be used to indicate critical events during walking (i.e., HS, FF, PO and TO). In the system, it is programmed that when the physical PO is detected by force sensors, the system switches to the swing phase without an indication from the phase variable. By using two independent sources of walking detection, the users can have more reliable gait with the prosthesis on various slopes.

III. UNIFIED CONTROL FRAMEWORK FOR SLOPE WALKING

The powered prosthetic system is operated with a control framework illustrated in Fig. 3. At the highest level, the micro-processor determines the appropriate walking state using the phase variable and force sensors to detect the user intention during walking. Depending on the determined state, the mid-level controller calculates the desired torques and communicates with the motor drivers. At the lowest level, the system implements torque control by modulating current to the motors for each joint. In this section, we focus on mid-level control strategies: impedance control and trajectory tracking. Especially, a unified trajectory generation for different slope conditions during the swing phase is addressed and discussed.

A. Impedance based controller

To successfully control the system during the stance phase, the impedance-based approach is suggested rather than trajectory tracking. The torque at each joint can be described by the following function consisting of a virtual angular stiffness (k_i), damping parameter (b_i), and the equilibrium angle (θ_i^{eq}), where $i \in \{\mathbf{a}nkle, \mathbf{k}nee\}$.

$$\tau_i = k_i(\theta_i - \theta_i^{eq}) + b_i\dot{\theta}_i \tag{1}$$

According to the previous research [22], [23], the mechanical impedance of human joints vary while walking. In order to enforce this idea to the prosthetic system, the human gait is usually separated into several stages. Some researchers use different constant impedance values for each stage [22], [23], other researchers use piece-wise functions to represent the ankle impedance during the human walking gait cycle [11], [18]. While the previous studies constrain the joint impedance parameters to be constant within a given state [22], [23], the impedance values used during the stance phase in this study can be described as functions of the phase variable – the virtual angular stiffnesses (k_a, k_k) are set linearly increase, and the damping of the ankle (b_a) to

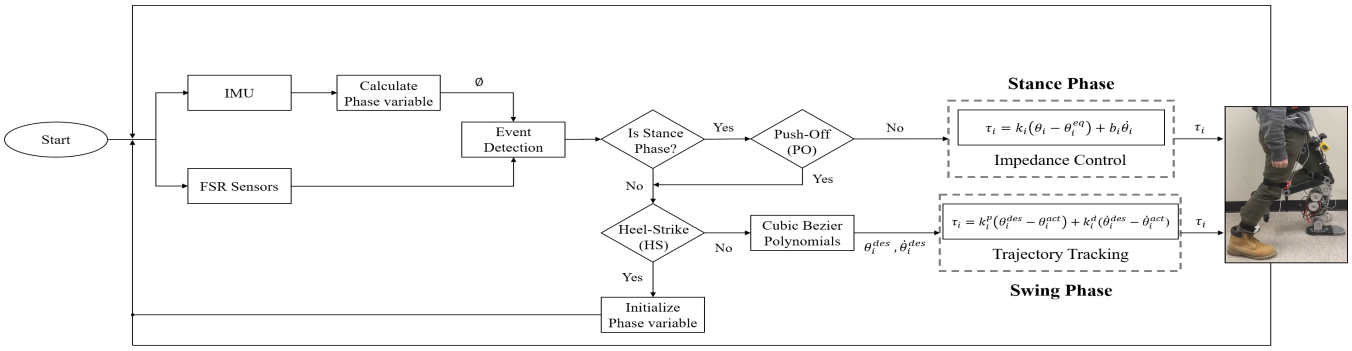

Fig. 3: The systemic flow of the prosthesis is illustrated above. The phase variable $\phi \in [0,1]$ is calculated from IMU data. Event detector (i.e., the information from both IMU and force sensors) determines the gait phase: stance or swing. $\theta_i^{des}, \dot{\theta}_i^{des}$, $\theta_i^{act}, \dot{\theta}_i^{act}$ indicate the desired joint angle, angular velocity and the actual joint angle, angular velocity respectively, where $i \in \{\mathbf{a}nkle, \mathbf{k}nee\}$.

linearly decrease, while the damping for the knee (b_k) is set to be constant. Though the final equilibrium angles of the ankle and knee (θ_a^{eq}, θ_k^{eq}) were considered to decrease to -12° and -45° respectively during the swing phase according to [5], the equilibrium angles in this case are set to 0° and -5° since we only use the impedance parameters for the stance phase.

B. Cubic Bezier polynomials based optimization

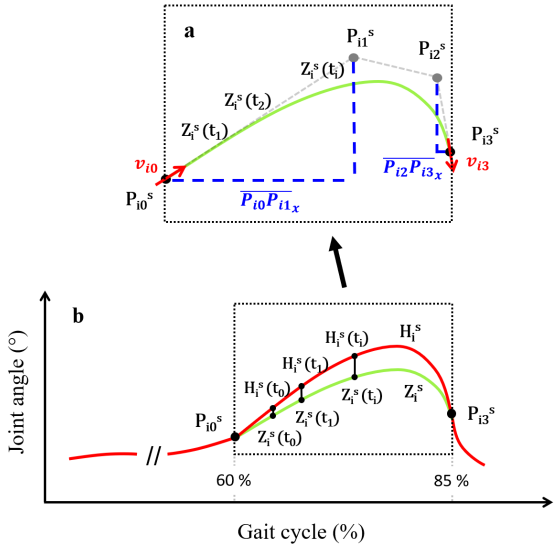

Fig. 4: (a) Cubic Bezier polynomial with control points ($P_{i0}^s - P_{i3}^s$). When P_{i0}^s, P_{i3}^s are fixed, depending on the control points P_{i1}^s and P_{i2}^s, the final curvature $Z_i^s(t)$ varies dramatically. (b) Based on $Z_i^s(t)$, human slope walking optimization was performed comparing to the human data (H_i^s) for both joints, where $i \in \{\mathbf{a}nkle, \mathbf{k}nee\}$ and $s \in \{-15°, -10°, -5°, 0°, 5°, 10°, 15°\}$. Note that the trajectory shown in the figure is not indicating any specific joint, but an arbitrary trajectory for explaining the concept.

During the swing phase, to guarantee a sufficient foot clearance (especially for the downslope walking), the proper walking trajectories according to the inclination are required. In order to generate the proper trajectories during the swing phase, 3^{rd} order Bezier polynomials are used as the base function, where $t \in [0,1]$ which is related to the gait cycle (60% – 85%) and the control points ($P_{i0}^s - P_{i3}^s$) are corresponding to the proper joint angles :

$$Z_i^s(t) = (1-t)^3 P_{i0}^s + 3t(1-t)^2 P_{i1}^s + 3t^2(1-t)P_{i2}^s + t^3 P_{i3}^s \quad (2)$$

According to the geometric relationship between the control points of Bezier polynomials in Fig. 4a, P_{i1}^s and P_{i2}^s can be re-described using $P_{i0}^s, P_{i3}^s, v_{i0}, v_{i3}$ as below, where $\overline{P_{i0}P_{i1_x}}$ and $\overline{P_{i2}P_{i3_x}}$ are the horizontal projections of $\overline{P_{i0}P_{i1}}$ and $\overline{P_{i2}P_{i3}}$, respectively :

$$\begin{aligned} P_{i1}^s &= (P_{i0}^s + \overline{P_{i0}P_{i1_x}} v_{i0}) \\ P_{i2}^s &= (P_{i3}^s - \overline{P_{i2}P_{i3_x}} v_{i3}) \end{aligned} \quad (3)$$

Based on the human observation in Fig. 1, the underlying assumptions are considered that i) at 60% of the gait cycle, the gradient of joint angle (v_{i0}) on the different slopes seem to be the same regardless of the slopes, ii) at 85% of the gait cycle, all slope walking trajectories are converging into the same joint position (P_{i3}^s) with the identical gradient of joint angle (v_{i3}) and iii) the same $\overline{P_{i0}P_{i1_x}}$, $\overline{P_{i2}P_{i3_x}}$ are used for all slope walking trajectories. Note that the proper joint positions at PO (P_{i0}^s), at 85% of gait cycle (P_{i3}^s) and their velocities (v_{i0}, v_{i3}) are given beforehand based on the human data while solving the problem.

To get closer slope walking trajectories to human walking, an offline optimization problem was defined to minimize the error between the Bezier curves (Z_i^s) and the human data (H_i^s) shown in Fig. 4b :

$$\begin{aligned} \min_{x_{i1},\, x_{i2}} \quad & f = \sum_s ||Z_i^s(t) - H_i^s(\phi)|| \\ s.t \quad & Z_i^s(0) = H_i^s(0.60) = P_{i0}^s \quad ,\forall s \\ & Z_i^s(1) = H_i^s(0.85) = P_{i3}^s \quad ,\forall s \\ & \dot{Z}_i^s(0) = \dot{H}_i^s(0.60) = v_{i0} \quad ,\forall s \\ & \dot{Z}_i^s(1) = \dot{H}_i^s(0.85) = v_{i3} \quad ,\forall s \end{aligned} \quad (4)$$

TABLE I: Optimized coefficients for Bezier curve with the correlation of 0.9818 (ankle) and 0.9976 (knee) comparing to human data during 60% - 85% of the gait cycle

Coefficients	Ankle (i:=a)	Knee (i:=k)
x_{i1}	0.1122	0.0617
x_{i2}	0.1170	0.0568

While satisfying the boundary constraints, Euclidean norm was used to find the optimal values which can minimize the defined objective function in Eq. 4. In this problem, from the vector $X_i := [x_{i0},\ x_{i1},\ x_{i2},\ x_{i3}]^T = [P_{i0},\ \overline{P_{i0}P_{i1}}_x,\ \overline{P_{i2}P_{i3}}_x,\ P_{i3}]^T$, only x_{i1} and x_{i2} were treated as the free variables since $[x_{i0}, x_{i3}]^T = [P_{i0}, P_{i3}]^T$ were given by the assumption. This Eq. 4 is handled as an offline optimization problem using MATLAB. The optimal coefficients from the optimization problem have been presented in Table I. In the prosthetic system, P_{i3} and v_{i3} are given from the human observation while the initial point (P_{i0}) and velocity (v_{i0}) are updated for every gait cycle by the sensor data with high correlation (Table I). Using these coefficients, Bezier curve trajectories can be generated in real-time without mandating online optimization.

IV. EXPERIMENTAL IMPLEMENTATION

A. Powered Transfemoral Prosthesis

AMPRO II is the second generation powered transfemoral prosthetic system custom-designed at Texas A&M University. It is fully actuated with two Brushless DC (BLDC) motors (MOOG, BN28) positioned at the ankle and knee. *AMPRO II* is operated by a 3-layered control framework that tracks the generated joint angle trajectories in accordance with the user's gait progression, which is determined by a phase variable calculated based on the global thigh angle measured by a 9-axis Inertia Measurement Unit (IMU) on the prosthesis. Force sensors (Tekscan, FlexForce) underneath the prosthetic foot are also utilized to detect walking events (i.e., heel-strike or push-off) for switching from stance phase to swing phase, and vice versa. During operation, the IMU processor and high-level control (implemented by two element14, BeagleBone Black operating at 200Hz) are used to calculate the phase variable and the corresponding walking state. Depending on the estimated walking state, the mid-level controller calculates the desired torques and transmits them to the motor drivers (ELMO, G-SOLWHI); these motor drivers control the two actuators via Controller Area Network (CAN) protocol at the lowest level. The actual joint angle data are captured by two high-resolution optical encoders (US Digital, E5) on the prosthesis.

In order to provide both compliance and pushing force to the prosthetic foot, we divided the foot into two parts (i.e., toe and foot-base) and connected them using a hinge and spring steel (Fig. 5). The hinge acts as a toe joint, and the spring steel on the foot can provide the elastic restoring force to the system during PO. The location of the toe joint was determined based on the human factor [20] (i.e., where the foot bends with respect to the entire foot). According

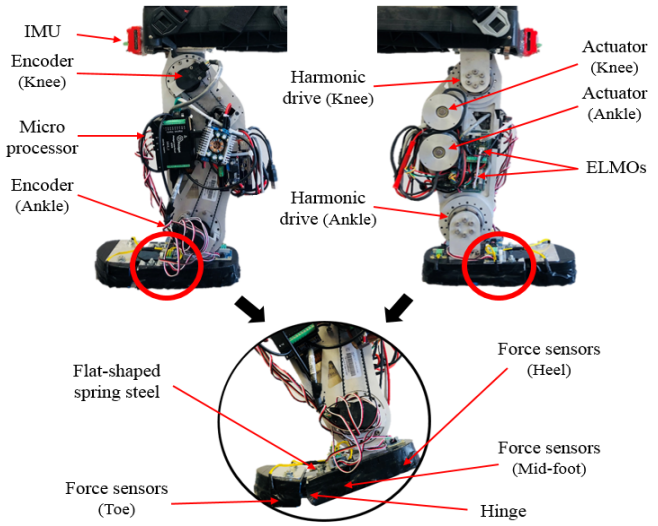

Fig. 5: *AMPRO II* is comprised on an actuated knee and ankle and a passive toe joint.

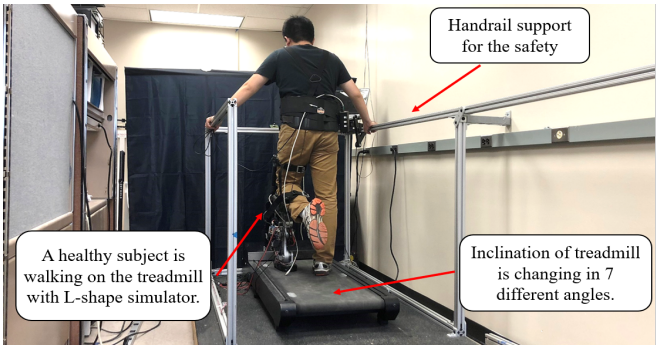

Fig. 6: The preliminary experiment with the able-bodied subject was conducted on the treadmill in seven different slopes. During the experiment, the safety issue was handled with the handrail support along the walkway under the supervisor.

to Winter [30], forefoot strike occurs with a striking index between 0.67 and 1.00 during running; strike index 0 refers to the end of the heel and 1.00 refers to the tip of the toe. The stiffness of the toe joint can be modulated by changing the number of spring steel sheets. In this research, we applied three layers of spring steel which is corresponding to 9 Nm/rad stiffness [8].

B. Experimental setup & protocol

To validate that the prosthetic system successfully meets the needs for sloped walking, an indoor experiment was designed as shown in Fig. 6. The experiment was conducted on a treadmill with handrails installed along the sides to assure the safety of the subject. The experimental protocol was reviewed and approved by the Institutional Review Board (IRB) at Texas A&M University (IRB2015-0607F).

A healthy subject (male, 5'7" height, 150lb weight) participated in the experiment with the L-shape simulator that attached to the prosthetic. The subject was asked to walk on

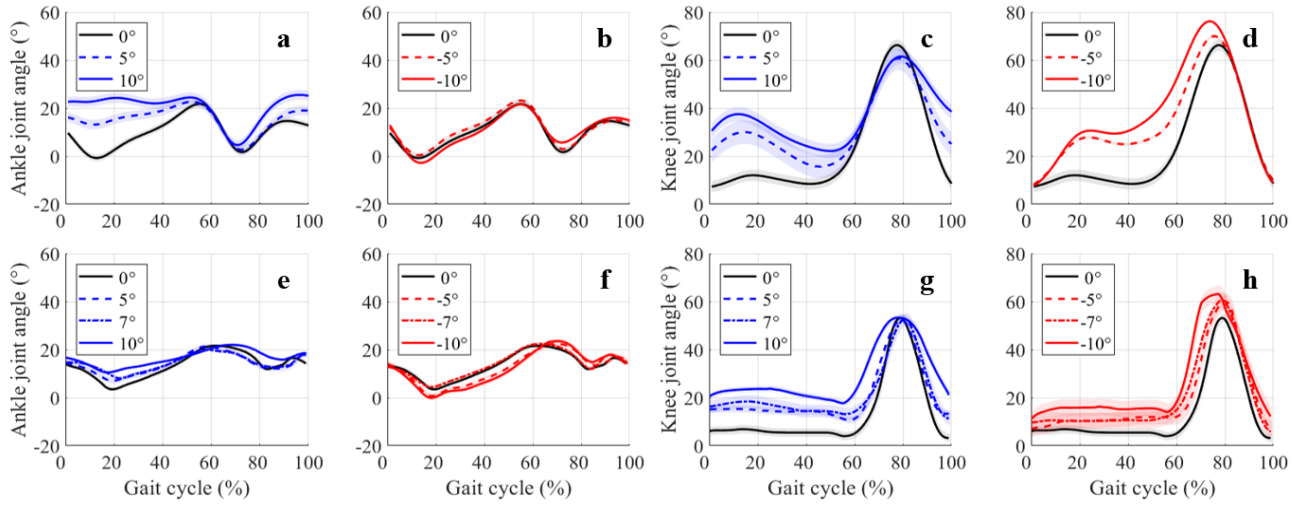

Fig. 7: The comparison between the human data (a - d) and the prosthetic data (e - h) from the encoder on both joints for a single gait cycle. All the bold lines in the prosthetic results indicate are the average of five steps performed by the subject while the shades indicate ± 1 standard deviation. Note that the results on $\pm 7°$ slope are shown only in the prosthesis' result since the corresponding human data were not collected.

a treadmill at seven different slopes: -10°, -7°, -5°, 0°, 5°, 7° and 10°. The experiment was not conducted on the $\pm 15°$ slope due to the physical limitation of the prosthesis's design; the range of knee joint angle was limited to maximum 63° with a L-shape simulator. The treadmill speed was based on the user's comfort (1.71 km/h) and all joint kinematic data of the subject was captured using the encoders on the prosthesis.

C. Experimental results and discussion

The encoder data from the experiment for a single gait cycle is indicated in Fig. 7. Fig. 7e-h show that both ankle and knee joint trajectories have qualitatively similar walking compared to human slope walking trajectories (Fig. 7a-d). Specifically, at the knee joint, compliant walking during the stance phase and the enlarged flexion depending on the downslope during the swing phase are clearly shown. However, it is shown that the knee joint angle has a relatively large difference compared to the human results. This is because the aforementioned hardware limitation to the knee joint mainly causes the joint angle difference from to the human data. From the supplemental video result [31], we would check the enlarged knee flexion by tracking the desired Bezier trajectory can avoid the collision with the slope even though it has less flexion compared to the human data. At the ankle joint, as the slope increases the initial joint angle increases. This is also seen in the human data although, in the prosthesis, these differences are not as great. Also, for both upslope and downslope, PO can be observed in the prosthetic walking even though this is not as great as human walking. Differences between human walking and prosthesis walking can be due to a variety of reasons. Since the experiment was conducted with the able-bodied subject, using a simulator could affect the subject's gait itself which is related to the difference from human data. The joint angle differences during the stance phase can be improved by a tuning process to provide better impedance parameters. This also can improve the result at swing phase because the proposed method can be varying depending on the initial conditions at PO.

V. CONCLUSIONS

The proposed framework for slope walking allows the transfemoral prosthesis to overcome some difficulties of slope walking in real-time. Regardless of the slope information, appropriate joint trajectories can be generated from the suggested algorithm and can be tracked using a tuned PD controller during the swing phase. An impedance controller is implemented for the stance phase which enables the user to adapt to the slope more easily. During the swing phase, the prosthesis requires the proper joint angle trajectories to avoid a possible collision with the slope. This is achieved in this study by using cubic Bezier polynomials to provide enough flexibility to generate different joint trajectories as the inclination varies. By solving an offline optimization with the Bezier polynomials, the optimized parameters have a benefit to unify the trajectory generation process without prior knowledge of slope – resulting in a fast trajectory generation with proper foot clearance. Future work can be dedicated to improving the comfort and functionality of the prosthesis. Specifically, we plan to deeply examine how the effect of push-off changes when the stiffness of the toe joint or the cushioning material under the foot changes. Furthermore, to achieve a rigorous agreement about the stability, we plan to generate the walking gait using trajectory optimization to generate the walking motion with multi-contact phase [2], which can be achieved by incorporating the human and prosthesis models.

REFERENCES

[1] A. D. Ames. First Steps toward Automatically Generating Bipedal Robotic Walking from Human Data. pages 89–116. Springer, London, 2012.

[2] K. Chao and P. Hur. A step towards generating human-like walking gait via trajectory optimization through contact for a bipedal robot with one-sided springs on toes. In *IEEE/RSJ International Conference on Intelligent Robots and Systems (IROS)*, pages 4848–4853, Vancouver, BC, Canada, 2017.

[3] T. R. Dillingham, L. E. Pezzin, and E. J. MacKenzie. Limb amputation and limb deficiency: epidemiology and recent trends in the United States. *Southern Medical Journal*, 95(8):875–83, 2002.

[4] P. Ephraim and L. Duncan. People with amputation speak out. https://www.amputee-coalition.org/wp-content/uploads/2014/11/lsp_people-speak-out_120115-113243.pdf.

[5] N. P. Fey, A. M. Simon, A. J. Young, and L. J. Hargrove. Controlling knee swing initiation and ankle plantarflexion with an active prosthesis on level and inclined surfaces at variable walking speeds. *IEEE Journal of Translational Engineering in Health and Medicine*, 2:1–12, 2014.

[6] J. R. Franz, N. E. Lyddon, and R. Kram. Mechanical work performed by the individual legs during uphill and downhill walking. *Journal of Biomechanics*, 45(2):257–262, 2012.

[7] W. Hong and P. Hur. Transfemoral prosthesis control for slope walking with principal component analysis. In *American Society of Biomechanics (ASB)*, pages 1–2, Boulder, CO, USA, Aug. 2017.

[8] W. Hong, S. Patrick, and P. Hur. Effect of toe stiffness on the push-off and joint trajectories for the powered transfemoral prosthesis: A pilot study. In *American Society of Biomechanics (ASB)*, pages 1–2, Rochester, MN, USA, 2018.

[9] M. Kuster, S. Sakurai, and G. Wood. Kinematic and kinetic comparison of downhill and level walking. *Clinical Biomechanics*, 10(2):79–84, 1995.

[10] B. E. Lawson, H. A. Varol, A. Huff, E. Erdemir, and M. Goldfarb. Control of stair ascent and descent with a powered transfemoral prosthesis. *IEEE Transactions on Neural Systems and Rehabilitation Engineering*, 21(3):466–473, 2013.

[11] H. Lee, E. J. Rouse, and H. I. Krebs. Summary of human ankle mechanical impedance during walking. *IEEE Journal of Translational Engineering in Health and Medicine*, 4:1–7, 2016.

[12] A. S. McIntosh, K. T. Beatty, L. N. Dwan, and D. R. Vickers. Gait dynamics on an inclined walkway. *Journal of Biomechanics*, 39(13):2491–2502, 2006.

[13] D. C. Morgenroth, M. Roland, A. L. Pruziner, and J. M. Czerniecki. Transfemoral amputee intact limb loading and compensatory gait mechanics during down slope ambulation and the effect of prosthetic knee mechanisms. *Clinical Biomechanics*, 55:65–72, 2018.

[14] V. Paredes, W. Hong, S. Patrick, and P. Hur. Upslope walking with transfemoral prosthesis using optimization based spline generation. In *IEEE/RSJ International Conference on Intelligent Robots and Systems (IROS)*, pages 3204–3211, 2016.

[15] N. T. Pickle, A. M. Grabowski, J. R. Jeffers, and A. K. Silverman. The functional roles of muscles, passive prostheses, and powered prostheses during sloped walking in people with a transtibial amputation. *Journal of Biomechanical Engineering*, 139(11):111005, 2017.

[16] N. T. Pickle, J. M. Wilken, J. M. Aldridge Whitehead, and A. K. Silverman. Whole-body angular momentum during sloped walking using passive and powered lower-limb prostheses. *Journal of Biomechanics*, 49(14):3397–3406, 2016.

[17] D. Quintero, D. J. Villarreal, D. J. Lambert, S. Kapp, and R. D. Gregg. Continuous-phase control of a powered kneeankle prosthesis: Amputee experiments across speeds and inclines. *IEEE Transactions on Robotics*, 34(3):686–701, 2018.

[18] E. J. Rouse, L. J. Hargrove, E. J. Perreault, and T. A. Kuiken. Estimation of human ankle impedance during walking using the perturberator robot. In *IEEE RAS & EMBS International Conference on Biomedical Robotics and Biomechatronics (BioRob)*, pages 373–378, Jun. 2012.

[19] Serious Law LLP. Effects of amputation. http://www.seriousinjurylaw.co.uk/other-serious-claims/amputation/effects-of-amputation/.

[20] Sesamoiditis. Sesamoid bone. http://sesamoiditis.net/sesamoid-bone/.

[21] D. G. Smith. The transfemoral amputation level, part 1 - amputee coalition. http://www.amputee-coalition.org/resources/transfemoral-amputation-part-1/.

[22] F. Sup, A. Bohara, and M. Goldfarb. Design and control of a powered transfemoral prosthesis. *The International Journal of Robotics Research*, 27(2):263–273, 2008.

[23] F. Sup, H. A. Varol, and M. Goldfarb. Upslope walking with a powered knee and ankle prosthesis: Initial results with an amputee subject. *IEEE Transactions on Neural Systems and Rehabilitation Engineering*, 19(1):71–78, 2011.

[24] R. Tranberg. *Analysis of body motions based on optical markers Accuracy, error analysis and clinical applications*. PhD thesis, University of Gothenburg, 2010.

[25] C. L. Vaughan, B. L. Davis, and J. C. Oconnor. *Dynamics of Human Gait*. Kiboho Publishers, 1999.

[26] D. J. Villarreal and R. D. Gregg. A survey of phase variable candidates of human locomotion. *International Conference of the IEEE Engineering in Medicine and Biology Society, (EMBC)*, pages 4017–4021, 2014.

[27] D. J. Villarreal and R. D. Gregg. Unified phase variables of relative degree two for human locomotion. *International Conference of the Ieee Engineering in Medicine and Biology Society (EMBC)*, pages 6262–6267, 2016.

[28] D. J. Villarreal, D. Quintero, and R. D. Gregg. Piecewise and unified phase variables in the control of a powered prosthetic leg. *IEEE International Conference on Rehabilitation Robotics (ICORR)*, pages 1425–1430, 2017.

[29] A. Vrieling, H. van Keeken, T. Schoppen, E. Otten, J. Halbertsma, A. Hof, and K. Postema. Uphill and downhill walking in unilateral lower limb amputees. *Gait & Posture*, 28(2):235–242, 2008.

[30] D. Winter. *Biomechanics and Motor Control of Human Movement*. Wiley, 2009.

[31] Woolim Hong. The supplemental video for the powered transfemoral prosthetic walking on the sloped terrains. https://youtu.be/Z8TrcWyknzE.

[32] H. Zhao, J. Reher, J. Horn, V. Paredes, and A. D. Ames. Demonstration of locomotion with the powered prosthesis AMPRO utilizing online optimization-based control. In *International Conference on Hybrid Systems: Computation and Control*, pages 305–306, 2015.